

## Research Article

# Numerical Simulation of Axion Quintessence

**Carl L. Gardner**

*School of Mathematical & Statistical Sciences, Arizona State University, Tempe, AZ 85287-1804, USA*

Correspondence should be addressed to Carl L. Gardner, [carl.gardner@asu.edu](mailto:carl.gardner@asu.edu)

Received 20 March 2012; Accepted 12 June 2012

Academic Editor: Emilio Elizalde

Copyright © 2012 Carl L. Gardner. This is an open access article distributed under the Creative Commons Attribution License, which permits unrestricted use, distribution, and reproduction in any medium, provided the original work is properly cited.

Robust, scaled cosmological equations are derived for simulating the evolution of the scalar field, the scale factor, and the Hubble parameter during both expanding and contracting phases of the universe. These scaled equations are applied to both stable (always expanding universe) and unstable axion quintessence (expanding and then collapsing universe). When applied to unstable axion quintessence, these scaled equations allow the simulations presented here to proceed much closer to the singularity at the end of a collapsing universe than any previous simulations.

## 1. Introduction

Typically in quintessence theories with an asymptotically vanishing effective cosmological constant, the energy contrast in dark energy  $\Omega_{\text{DE}}$  rises from near zero for redshifts  $z > 5$  to near one for  $z < -0.5$ , mimicking a true cosmological constant. At late times, the quintessence field may begin to oscillate about its minimum, behaving like nonrelativistic matter, or the quintessence field may evolve toward infinity—in both cases with vanishing vacuum energy. In such theories, there is a period between roughly 3.5 Gyr and 20 Gyr after the big bang when  $0.1 \leq \Omega_{\text{DE}} \leq 0.9$ . However, if the universe continues to expand forever, or even if positive curvature begins to dominate at late times (after the quintessence field has evolved to its minimum) and the universe enters a contracting stage, this period when the energy densities of dark energy and matter are comparable is a small or vanishing fraction of the total lifetime of the universe. This is called the cosmic coincidence problem.

However in axion quintessence (as in other unstable de Sitter quintessence models), the cosmological era with  $0.1 \leq \Omega_{\text{DE}} \leq 0.9$  may represent a significant fraction of the universe's lifetime if the minimum of the axion potential is negative (unstable [de Sitter] axion quintessence), thus resolving [1] the cosmic coincidence problem. (Negative  $\rho_{\Lambda}$  or  $\rho_{\text{DE}}$  and the fate of the universe are discussed in [1] plus references therein.)

The unstable axion quintessence potential  $V(\varphi) = A \cos(\varphi)$ , where  $\varphi \equiv \phi/M_P$  and the Planck mass  $M_P = 1/\sqrt{8\pi G} = 2.4 \times 10^{18}$  GeV, addresses the main drawbacks of quintessence models, since the facts that the minimum of the potential is at  $-A \approx -\rho_\Lambda$ ,  $\rho_{\text{DE},0} = \rho_\Lambda$ , and  $w_0 \neq -1$  but  $\approx -1$  are interrelated aspects of the model, and they occur for an appreciable range of initial values for  $\phi$  (the subscript “0” denotes present values).

For  $V(\varphi) = A \cos(\varphi)$ , the initial value of the scalar field need only satisfy  $0 \leq \varphi_i/\pi \leq 0.23$  to produce a universe like ours [2] (due to symmetry, we can restrict our attention to  $0 \leq \varphi_i \leq \pi$ ). Thus, there is a significant 23% range of the possible initial values  $\varphi_i$  which will produce a universe like ours. (Qualitatively similar results to those presented here are obtained for  $V(\varphi) = A \cos(\lambda\varphi)$  for  $\lambda = O(1)$ .) For these initial values, the contracting universe enters a late time era of kination (during which the scalar field kinetic energy dominates over all other forms of energy)—the negative Hubble parameter acting like a negative friction term in the Klein-Gordon equation—and the axion field makes many transits of (but never remains in) its vacuum state. (The coupling of the quintessence field to other particles must be very small and will for the most part be neglected in this investigation.)

In Section 2, the basic cosmological equations are presented for the evolution of the scalar field, the scale factor, and the Hubble parameter, and cast in the form of a scaled, dimensionless system of first-order equations in the conformal time, appropriate for a contracting (or expanding) universe. These equations allow the simulations of unstable axion quintessence presented in Section 3 (see Figures 6–9) to proceed much closer to the singularity at the end of the collapsing universe than any other simulations presented in the literature and provide the basis for a more detailed analysis of the last stages of the collapsing universe than has appeared before. We also present simulations of stable axion quintessence  $V(\varphi) = A(1 + \cos(\varphi))$  which produce a universe like ours—and where asymptotically  $\Omega_{\text{DE}}$  saturates near  $\Omega_{\text{DE},0}$  for  $0.40 \leq \varphi_i/\pi \leq 0.52$ .

## 2. Cosmological Equations

In the quintessence/cold dark matter (QCDM) model, the total energy density  $\rho = \rho_m + \rho_r + \rho_\phi$ , where  $\rho_m$ ,  $\rho_r$ , and  $\rho_\phi$  are the energy densities in (nonrelativistic) matter, radiation, and the axion quintessence scalar field  $\phi$ , respectively. Ratios of energy densities to the critical energy density  $\rho_c$  for a flat universe will be denoted by  $\Omega_m = \rho_m/\rho_c$ ,  $\Omega_r = \rho_r/\rho_c$ , and  $\Omega_\phi = \rho_\phi/\rho_c$ , while ratios of present energy densities  $\rho_{m0}$ ,  $\rho_{r0}$ , and  $\rho_{\phi0}$  to the present critical energy density  $\rho_{c0}$  will be denoted by  $\Omega_{m0}$ ,  $\Omega_{r0}$ , and  $\Omega_{\phi0}$ , respectively.  $\Omega_{\text{DE}}$  will denote

$$\Omega_{\text{DE}} = \begin{cases} \Omega_\Lambda, & \Lambda\text{CDM}, \\ \Omega_\phi, & \text{QCDM}, \end{cases} \quad \text{if } w_\phi < -\frac{1}{3}. \quad (2.1)$$

Using WMAP5 [3] central values, we will set  $\Omega_{\text{DE},0} = 0.72$ ,  $\Omega_{r0} = 8.5 \times 10^{-5}$ ,  $\Omega_{m0} = 1 - \Omega_{\text{DE},0} - \Omega_{r0} \approx 0.28$ , and  $\rho_{c0}^{1/4} = 2.5 \times 10^{-3}$  eV, with the present time  $t_0 = 13.73$  Gyr after the big bang for  $\Lambda\text{CDM}$ .

The homogeneous scalar field obeys the Klein-Gordon equation:

$$\ddot{\phi} + 3H\dot{\phi} = -\frac{dV}{d\phi} \equiv -V_\phi. \quad (2.2)$$

The evolution of the universe is described by the Friedmann equations for the Hubble parameter  $H = \dot{a}/a$  and the scale factor  $a(t)$ :

$$H^2 = \frac{\rho}{3M_p^2} - \frac{k}{a^2}, \quad (2.3)$$

$$\frac{\ddot{a}}{a} = -\frac{1}{6M_p^2}(\rho + 3P), \quad (2.4)$$

where the energy density  $\rho = \rho_\phi + \rho_m + \rho_r$  and the pressure  $P = P_\phi + P_m + P_r$ , with  $P_m = 0$ ,  $P_r = \rho_r/3$ , and

$$\rho_\phi = \frac{1}{2}\dot{\phi}^2 + V(\phi), \quad P_\phi = \frac{1}{2}\dot{\phi}^2 - V(\phi). \quad (2.5)$$

The curvature signature  $k = +1, 0, -1$  for a closed, flat, or open geometry. Equation (2.4) shows that  $P < -\rho/3$  for an accelerating universe.

The conservation of energy equation for matter, radiation, and the scalar field is

$$\dot{\rho} + 3H(\rho + P) = 0. \quad (2.6)$$

Equation (2.6) gives the evolution of  $\rho_m$  and  $\rho_r$ , and with (2.5) the Klein-Gordon equation (2.2) for the weakly coupled scalar field. The time rate of change of the Hubble parameter is given by

$$\dot{H} = -\frac{\rho + P}{2M_p^2} + \frac{k}{a^2}. \quad (2.7)$$

Only two of (2.3), (2.4), (2.6), and (2.7) are independent. We will assume a flat universe after inflation and henceforth set  $k = 0$ .

The logarithmic time variable (number of  $e$ -folds of the scale factor) is defined as  $\tau = \ln(a/a_0) = -\ln(1+z)$ . Note that for de Sitter space  $\tau = H_\Lambda t$ , where  $H_\Lambda^2 = \rho_\Lambda/(3M_p^2)$ , and that  $H_\Lambda t$  is a natural time variable for the era of  $\Lambda$ -matter domination (see, e.g., [4]). We will make the simple approximations:

$$\rho_r = \rho_{r0}e^{-4\tau}, \quad \rho_m = \rho_{m0}e^{-3\tau}. \quad (2.8)$$

The equation of state parameter for the scalar field  $\phi$  is  $w_\phi = P_\phi/\rho_\phi$ . Since  $\tau$  is a natural time variable for the era of  $\Lambda$ -matter domination, we define the recent average of  $w_\phi$  as

$$w_0 = \frac{1}{\tau} \int_0^\tau w_\phi d\tau. \quad (2.9)$$

We will take the upper limit of integration to correspond to  $z = 1.75$ . The SNe Ia observations [5] bound the recent average  $-1.1 < w_0 < -0.85$  (95% CL).

For numerical simulations, the cosmological equations should be put into a scaled, dimensionless form. Equations (2.2) and (2.3) can be cast [2] in the form of a system of two first-order equations in  $\tau$  plus a scaled version of  $H$ :

$$\begin{aligned}\widetilde{H}\frac{d\varphi}{d\tau} &= \psi, \\ \widetilde{H}\left(\frac{d\psi}{d\tau} + \psi\right) &= -3\widetilde{V}_\varphi \\ \widetilde{H}^2 &= \widetilde{\rho}, \\ \widetilde{\rho} &= \frac{1}{6}\psi^2 + \widetilde{V} + \widetilde{\rho}_m + \widetilde{\rho}_r,\end{aligned}\tag{2.10}$$

where  $\varphi \equiv \phi/M_P$ ,  $\psi \equiv e^{2\tau}\dot{\varphi}/H_0$ ,  $\widetilde{H} = e^{2\tau}H/H_0$ ,  $\widetilde{V} = e^{4\tau}V/\rho_{c0}$ ,  $\widetilde{V}_\varphi = e^{4\tau}V_\varphi/\rho_{c0}$ ,  $\widetilde{\rho} = e^{4\tau}\rho/\rho_{c0}$ ,  $\widetilde{\rho}_m = e^{4\tau}\rho_m/\rho_{c0} = \Omega_{m0}e^\tau$ , and  $\widetilde{\rho}_r = e^{4\tau}\rho_r/\rho_{c0} = \Omega_{r0}$ . This scaling results in a set of equations that is numerically more robust, especially near and before the time of big-bang nucleosynthesis (BBN)—see [2].

For a contracting phase (in which  $H$  goes through zero), a different set of equations and a different scaling should be used. Here, we will use the conformal time variable,

$$\eta = \int_0^t \frac{a_0 H_0}{a} dt,\tag{2.11}$$

where  $t = 0$  corresponds to the big bang.

Equations (2.2) and (2.7) can be cast in the form of a system of three first-order equations in  $\eta$ :

$$\begin{aligned}\frac{d\varphi}{d\eta} &= \psi, \\ \frac{d\psi}{d\eta} &= -2\overline{H}\psi - 3\overline{V}_\varphi, \\ \frac{d\overline{H}}{d\eta} &= -\frac{1}{2}(\overline{\rho} + 3\overline{P}) = -\frac{1}{3}\psi^2 + \overline{V} - \frac{\Omega_{m0}}{2}e^{-\tau} - \Omega_{r0}e^{-2\tau}, \\ \overline{\rho} &= \frac{1}{6}\psi^2 + \overline{V} + \overline{\rho}_m + \overline{\rho}_r, \quad \overline{P} = \frac{1}{6}\psi^2 - \overline{V} + \frac{1}{3}\overline{\rho}_r,\end{aligned}\tag{2.12}$$

where  $\varphi \equiv \phi/M_P$ ,  $\psi \equiv e^\tau\dot{\varphi}/H_0$ ,  $\overline{H} = e^\tau H/H_0$ ,  $\overline{V} = e^{2\tau}V/\rho_{c0}$ ,  $\overline{V}_\varphi = e^{2\tau}V_\varphi/\rho_{c0}$ ,  $\overline{\rho} = e^{2\tau}\rho/\rho_{c0}$ ,  $\overline{\rho}_m = e^{2\tau}\rho_m/\rho_{c0} = \Omega_{m0}e^{-\tau}$ , and  $\overline{\rho}_r = e^{2\tau}\rho_r/\rho_{c0} = e^{-2\tau}\Omega_{r0}$ . This scaling results in a set of numerically more robust equations, especially near the turn-around time  $t_*$  between expanding and contracting phases of the universe.

Note that the conformal time  $\eta$  is related to the logarithmic time  $\tau$  by

$$\frac{d\tau}{d\eta} = \overline{H}.\tag{2.14}$$

**Table 1:** Parameters for the potential  $V = A \cos(\varphi)$ .  $t_0$  is the current age of the universe with  $t_0 \equiv 13.73$  Gyr in the  $\Lambda$ CDM model,  $0.1 \leq \Omega_{\text{DE}} \leq 0.9$  for  $t_{0.1} \leq t \leq t_{0.9}$ , the “coincidence” time interval  $\Delta t_c = t_{0.9} - t_{0.1}$ ,  $t_*$  is the turn-around time,  $t_f$  is the time of the big crunch, and  $a_* = a(t_*)$ . All times are in Gyr. \*For  $\varphi_i/\pi = 0.20$  (0.23),  $\Omega_{\text{DE}} \leq 0.85$  (0.77) and in these cases  $t_{0.9} \equiv t_{0.85}$  and  $t_{0.77}$ , respectively.

$\varphi_i/\pi$	$A/\rho_{c0}$	$w_0$	$t_0$	$t_{0.1}$	$t_{0.9}$	$t_*$	$t_f$	$t_c/t_f$	$a_*/a_0$
0.05	0.73	-0.998	13.72	3.6	20.0	63.2	72.7	0.23	12.0
0.10	0.78	-0.99	13.70	3.5	20.3	47.6	56.8	0.30	5.0
0.15	0.88	-0.97	13.64	3.5	21.2	37.6	46.2	0.38	3.0
0.20	1.09	-0.93	13.49	3.3	21.2*	29.2	37.0	0.48	2.0
0.23	1.41	-0.87	13.25	3.0	16.8*	23.9	30.7	0.45	1.6

### 3. Simulations of Axion Quintessence

The original axion quintessence potential  $V = A(1 + \cos(\varphi))$  was based on  $N = 1$  supergravity [6, 7], with  $m_\phi^2 = 3H_\Lambda^2$ . As  $\varphi \rightarrow \pi$ , the universe evolves to Minkowski space.

The unstable de Sitter axion potential  $V = A \cos(\varphi)$  is based on M/string theory reduced to an effective  $N = 1$  supergravity theory [8], with  $m_\phi^2 = -3H_\Lambda^2$  at the maximum of  $V$ .

Both axion quintessence models are derivable (up to a constant) from string theory as axion monodromy [9].

The quintessence axion is a pseudo-Nambu-Goldstone boson: at the perturbative level the theory is shift symmetric under  $\varphi \rightarrow \varphi + \text{const}$  with  $\varphi = \phi/M$ . The shift symmetry is broken—before or during inflation—by nonperturbative instanton effects to a discrete symmetry  $\varphi \rightarrow \varphi + 2\pi$ , generating a potential  $V(\varphi) = A(C + \cos(\varphi))$ . In these theories, quantum corrections to the classical axion potential are suppressed. For quintessence (or for natural inflation [10]),  $M \sim M_P$ ; we will take  $M = M_P$ .  $C = 0$  and  $C = 1$  are the most interesting unstable axion and original axion cases, respectively.

#### 3.1. Unstable Axion Quintessence

For the unstable axion quintessence  $V = A \cos(\varphi)$  computations (with an expanding and then contracting universe), we will use (2.12) and (2.14) with initial conditions  $\varphi_i$  and  $\dot{\varphi}_i = 0$  specified at matter-radiation equality  $z_{mr} = 3280$ , which corresponds to

$$\eta_{mr} = \frac{2(\sqrt{2} - 1)}{\sqrt{\Omega_{m0}}\sqrt{1 + z_{mr}}}. \quad (3.1)$$

The constant  $A$  in the potential is adjusted so that  $\Omega_{\phi 0} = 0.72$ . This involves the usual single fine tuning. Note that the same anthropic arguments that limit the magnitude of a present-day cosmological constant also limit  $A < 100\rho_{c0}$ , so the tuning of  $A$  is no worse than the tuning of a cosmological constant.

Results for the unstable axion potential are presented in Table 1 for various  $\varphi_i$  and for  $\varphi_i/\pi = 0.1$  in Figures 1–9. (As  $\varphi_i \rightarrow 0$ , classically  $t_f \rightarrow \infty$ , but quantum effects destabilize

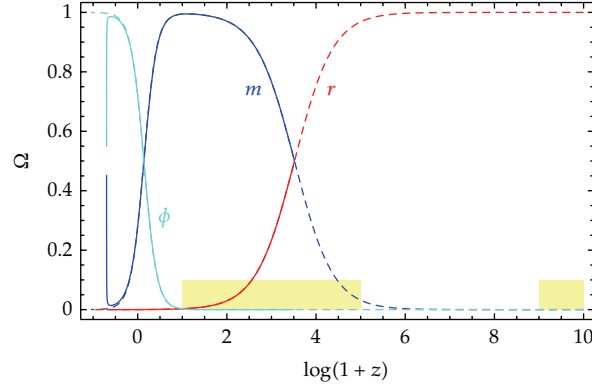


**Figure 1:**  $\Omega$  versus  $\log_{10}(1+z)$  for the potential  $V = A \cos(\varphi)$ ,  $\varphi_i/\pi = 0.1$  (solid) versus  $\Lambda$ CDM (dotted). The light yellow rectangles are the bounds on  $\Omega_{\text{DE}}$  from LSS, CMB, and BBN.

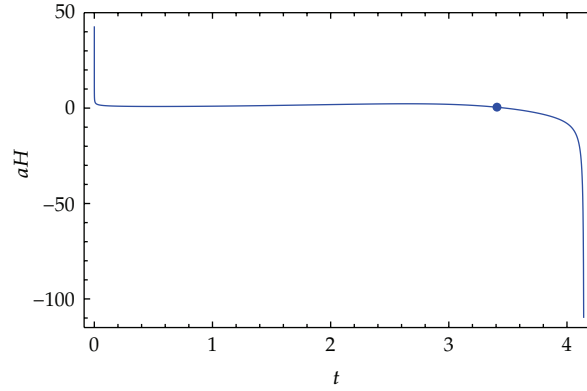


**Figure 2:** Comoving Hubble parameter  $aH/(a_0H_0)$  versus  $t/t_0$ . The dot indicates the value  $H = 0$  at  $t_*$ .

$\varphi_i \approx 0$  so that the maximum  $t_f \sim 100t_0$  [1].) For the values in the table, as  $\varphi_i$  increases,  $|V_\phi(\phi_i)|$  also increases and  $\phi$  starts to move earlier, leading to a decrease in  $t_{0.1}$ ,  $t_0$ ,  $t_*$ , and  $t_f$ , and correspondingly to an increase in  $w_0$  away from  $-1$ . Note that, for  $\varphi_i/\pi = 0.2$ , the coincidence time ratio approaches 50%.

The QCDM universe mimics the  $\Lambda$ CDM model (see Figure 1; for clarity, only the beginnings of the contracting stage are shown in this figure) until about  $z = -0.5$ , after which the QCDM universe begins to decelerate and ultimately to rapidly contract to a big crunch (Figures 2 and 3).

During the contracting stage,  $H < 0$  acts as a *negative* friction in

$$\ddot{\phi} + 3H\dot{\phi} + V_\phi = 0, \quad (3.2)$$

amplifying the axion field and its kinetic energy to bring about a late-stage kination era during which the scalar field kinetic energy dominates over all other forms of energy.

The quintessence axion is an ultra-light scalar field with  $m_\phi^2 \sim H_\Lambda^2$ , so  $\phi$  “sits and waits” during the early evolution of the universe, and it only starts to move when  $H^2 \sim m_\phi^2$

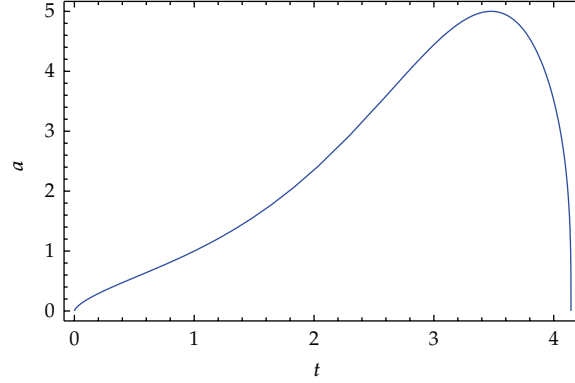


Figure 3: Scale factor  $a/a_0$  versus  $t/t_0$ .

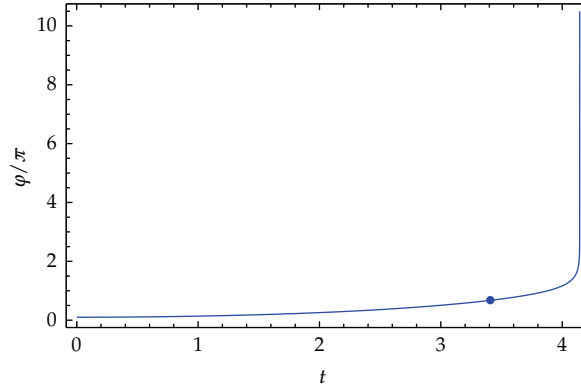
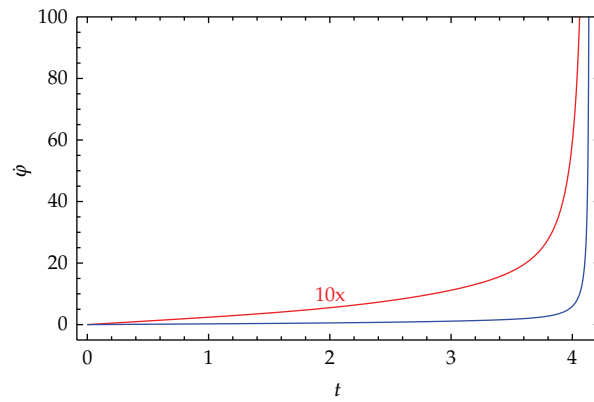


Figure 4:  $\varphi/\pi$  versus  $t/t_0$ . The dot indicates the value  $\varphi/\pi = 0.67$  at  $t_*$ .

(Figures 4 and 5). In this way, it is easy to satisfy the BBN ( $z \sim 10^9-10^{11}$ ), cosmic microwave background (CMB) ( $z \sim 10^3-10^5$ ), and large-scale structure (LSS) ( $z \sim 10-10^4$ ) bounds on  $\Omega_{DE} \lesssim 0.1$ , as in Figure 1. An ultra-light scalar field also reflects the observational evidence that the universe has only recently become dominated by dark energy.

In Figure 2, the Hubble parameter goes through zero at the turn-around time between an expanding and contracting universe. At the beginning of the contracting stage,  $\phi$  has yet to reach the minimum of the potential energy (see Figure 6), and thus the negative Hubble parameter amplifies the kinetic energy of the scalar field, bringing about an era of kination with  $w_\phi = 1$ , as seen in Figures 4, 5, 7, and 8. Also, note that Figures 2, 4, and 5 indicate that  $H$ ,  $\dot{\phi}$ , and  $\ddot{\phi}$  are approaching a singularity near  $t_f$ . In fact, in an era of kination during contraction during which  $H = -|\dot{\phi}|/(\sqrt{6}M_P)$ ,  $\dot{\phi} = \sqrt{2/3}M_P/(t_f - t)$ , and  $\varphi = -\sqrt{2/3} \ln(M_P(t_f - t))$ , while  $a \sim (t_f - t)^{1/3}$  (see Figure 3).

Figure 6 shows that as  $\phi$  increases without bound, the potential energy  $V(\phi)$ , since a periodic function of  $\phi$ , oscillates more and more rapidly. Depending on the strength of the coupling between the quintessence axion and other particles,  $\phi$  may decay and populate the universe with additional radiation and matter. (The monotonically increasing field  $\phi$  in a periodic potential can be interpreted as an oscillating field.) At the very least, there should be gravitational production of particles by  $\phi$  during contraction.



**Figure 5:**  $\dot{\phi}/H_0$  and  $10\dot{\phi}/H_0$  versus  $t/t_0$ .

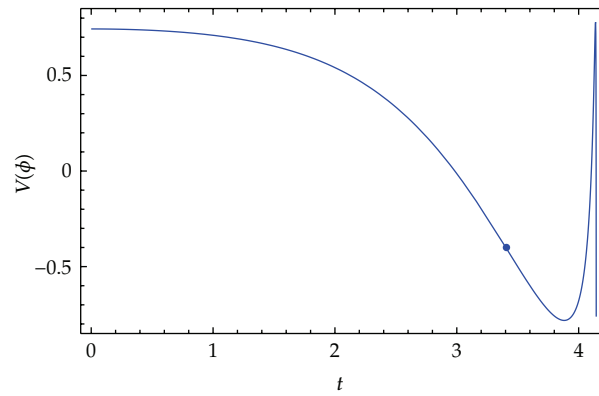


**Figure 6:** Potential  $V(\phi)/\rho_{c0}$  versus  $t/t_0$ . The dot indicates the value of  $V/\rho_{c0}$  at  $t_*$ .

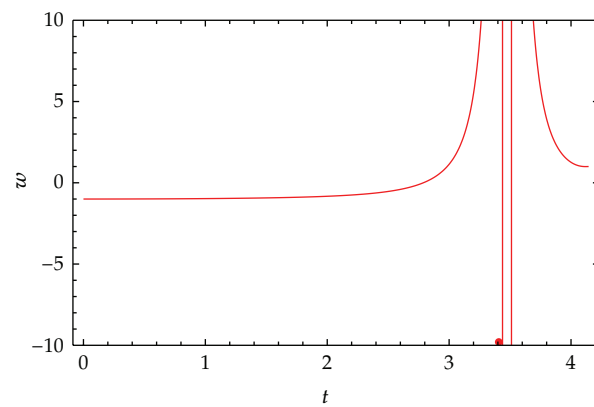


**Figure 7:**  $\omega_\phi$  versus  $t/t_0$ . The dot indicates  $t_*$ .



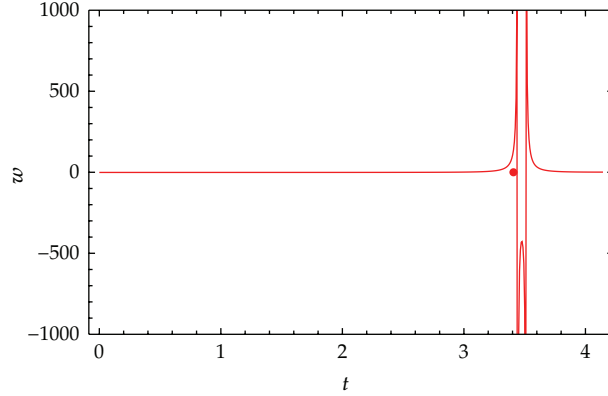


Figure 8: Overview of  $w_\phi$  versus  $t/t_0$ . The dot indicates  $t_*$ .

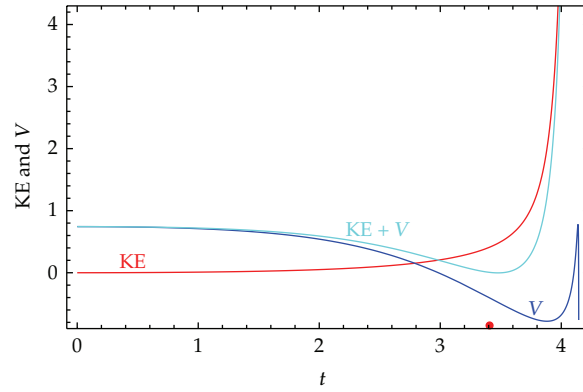


Figure 9: Scalar field kinetic energy density  $\dot{\phi}^2/2$  and potential energy density  $V(\phi)$  versus  $t/t_0$ . The dot indicates  $t_*$ .

Figures 7 and 8 follow the contracting stage further, illustrating that, although  $w_\phi \rightarrow \pm\infty$  twice just after  $t_*$ , the universe ultimately enters a stage of kination in which  $w_\phi = 1$  near  $t_f$ . Note that  $w_\phi \approx -1$  until well after  $t_0$ .

After matter-quintessence equality at  $t_{m\phi} \approx 0.7t_0$ , the scalar field energy density always dominates over the matter and radiation energy densities. There is a period from  $t \approx 2.5t_0$  until  $3.8t_0$  when the scalar field potential energy is comparable to its kinetic energy, and then the kinetic energy (which scales as  $1/a^6$ ) predominates during the rapid contraction to a big crunch (see Figure 9).

### 3.2. Stable Axion Quintessence

For the stable axion quintessence  $V = A(1 + \cos(\varphi))$  computations, we use the same equations (2.12) and (2.14) with initial conditions  $\varphi_i$  and  $\dot{\varphi}_i = 0$  also specified at matter-radiation equality. Again, the constant  $A$  in the potential is adjusted so that  $\Omega_{\phi 0} = 0.72$ .

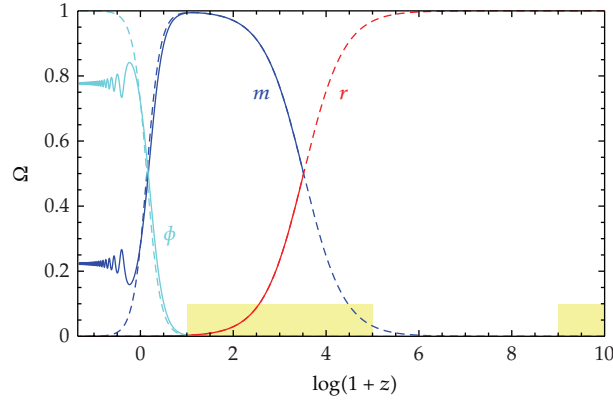


**Figure 10:**  $\Omega$  versus  $\log_{10}(1+z)$  for the potential  $V = A(1 + \cos(\varphi))$ ,  $\varphi_i/\pi = 0.5$  (solid) versus  $\Lambda$ CDM (dotted).

Simulations of stable axion quintessence are presented in [2]. As  $\varphi_i \rightarrow 0$ , a transient de Sitter universe is obtained that mimics the  $\Lambda$ CDM model for a long time. Near  $t_0$ ,  $\varphi$  is beginning to evolve toward  $\pi$ . The initial value of the scalar field needs only satisfy  $0 \leq \varphi_i/\pi \leq 0.52$  to produce a universe like ours [2]. Thus, there is a significant 52% range of the possible initial values  $\varphi_i$  which will produce a universe like ours.

For  $0.40 \leq \varphi_i/\pi \leq 0.52$ , stable axion quintessence not only produces a universe like ours, but  $\Omega_{\text{DE}}$  also asymptotically saturates near  $\Omega_{\text{DE},0}$  (Figure 10).

#### 4. Conclusion

In the unstable axion quintessence case, at late times, the contracting universe enters an era of kination in which  $\phi \sim -\ln(t_f - t)$ ,  $a \sim (t_f - t)^{1/3}$ , and  $H \sim (t_f - t)^{-1}$ . The density and pressure during this era scale as  $(t_f - t)^{-2}$ . The singularity behavior is analogous to the Type III singularity of [11, 12] in which as  $t \rightarrow t_f$ ,  $a \rightarrow a_s$ ,  $\rho \rightarrow \infty$ , and  $|P| \rightarrow \infty$ , except here  $a_s = 0$  (quantum effects though should stabilize  $a_s$  near  $1/M_P$ ).

As the universe contracts, density inhomogeneities are amplified and presumably black holes are formed, similarly to the contracting stage of the ekpyrotic universe [13] with  $w = 1$ . Depending on the strength of the coupling (which we have neglected here) between the quintessence axion and other particles,  $\phi$  may decay and produce radiation and matter. There should at least be gravitational production of particles by  $\phi$  during contraction. As the universe reheats during contraction, broken symmetries are restored. It is possible that inflating patches may be generated, spawning new universes from the old.

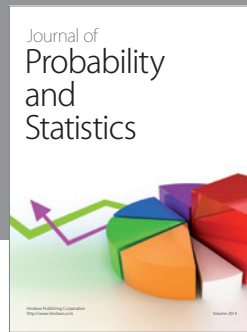
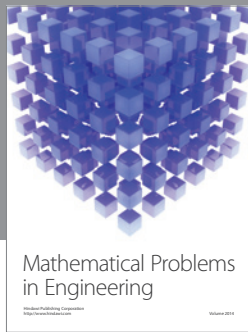
In summary, stable axion quintessence can produce a universe like ours, in which for  $0.40 \leq \varphi_i/\pi \leq 0.52$ ,  $\Omega_{\text{DE}}$  asymptotically saturates near  $\Omega_{\text{DE},0}$ . The unstable axion quintessence potential resolves the main drawbacks of quintessence: the minimum of the potential is not at zero, but at a negative value  $\approx -\rho_\Lambda$ ,  $\rho_{\text{DE},0} = \rho_\Lambda$  with only a single fine tuning (in the anthropic range), and  $w_0$  naturally satisfies  $-1 < w_0 \leq -0.87$ , for an appreciable 23% range of possible initial values for the quintessence field. And for a universe like ours, the coincidence time when the energy densities of dark energy and matter are comparable varies (as long as  $\phi_i/\pi$  is not too small—say,  $\geq 0.05$ ) from 25%–50% of the lifetime of the universe.

## Acknowledgment

The author's thanks are due to Lawrence Krauss for valuable comments.

## References

- [1] R. Kallosh, A. Linde, S. Prokushkin, and M. Shmakova, "Supergravity, dark energy, and the fate of the universe," *Physical Review D*, vol. 66, no. 12, Article ID 123503, 17 pages, 2002.
- [2] C. L. Gardner, "Quintessence and the transition to an accelerating universe," *Nuclear Physics B*, vol. 707, no. 1-2, pp. 278–300, 2005.
- [3] E. Komatsu, J. Dunkley, M. R. Nolte et al., "Five-year Wilkinson Microwave Anisotropy Probe (WMAP) observations: cosmological interpretation," *The Astrophysical Journal Supplement Series*, vol. 180, no. 2, p. 330, 2009.
- [4] C. L. Gardner, "Cosmological variation of the fine structure constant from an ultralight scalar field: the effects of mass," *Physical Review D*, vol. 68, no. 4, Article ID 043513, 7 pages, 2003.
- [5] A. G. Riess, L. G. Sirolder, J. Tonry et al., "Type Ia supernova discoveries at  $z > 1$  from the Hubble Space Telescope: evidence for past deceleration and constraints on dark energy evolution," *Astrophysical Journal*, vol. 607, no. 2, pp. 665–687, 2004.
- [6] J. A. Frieman, C. T. Hill, A. Stebbins, and I. Waga, "Cosmology with ultralight pseudo Nambu-Goldstone bosons," *Physical Review Letters*, vol. 75, no. 11, pp. 2077–2080, 1995.
- [7] I. Waga and J. A. Frieman, "New constraints from high redshift supernovae and lensing statistics upon scalar field cosmologies," *Physical Review D*, vol. 62, no. 4, Article ID 043521, 5 pages, 2000.
- [8] K. Choi, "String or M theory axion as a quintessence," *Physical Review D*, vol. 62, no. 4, Article ID 043509, 13 pages, 2000.
- [9] E. Silverstein and A. Westphal, "Monodromy in the CMB: gravity waves and string inflation," *Physical Review D*, vol. 78, no. 10, Article ID 106003, 21 pages, 2008.
- [10] K. Freese, C. Savage, and W. H. Kinney, "Natural inflation: status after WMAP three-year data," *International Journal of Modern Physics D*, vol. 17, no. 1, pp. 2573–2586, 2008.
- [11] S. Capozziello, M. De Laurentis, S. Nojiri, and S. D. Odintsov, "Classifying and avoiding singularities in the alternative gravity dark energy models," *Physical Review D*, vol. 79, no. 12, Article ID 124007, 16 pages, 2009.
- [12] S. Nojiri, S. D. Odintsov, and S. Tsujikawa, "Properties of singularities in the (phantom) dark energy universe," *Physical Review D*, vol. 71, no. 6, Article ID 063004, 16 pages, 2005.
- [13] J. L. Lehners, P. J. Steinhardt, and N. Turok, "The return of the phoenix universe," *International Journal of Modern Physics D*, vol. 18, no. 14, pp. 2231–2235, 2009.



# Hindawi

Submit your manuscripts at  
<http://www.hindawi.com>

